

## ABSTRACT

Glioblastomas are characterized by rapid cell growth, CNS infiltration, and are resistant to all known anticancer regimens. Therefore, development of new more effective therapies against these malignant brain tumors is the major challenge for modern medicine. Anti-neoplastic potential of fenofibrate is gaining a lot of attention. However, the precise mechanism/s of fenofibrate anti-tumoral action remain to be elucidated. Fenofibrate is a potent agonist of PPAR $\alpha$ , which is expected to shift energy metabolism from glycolysis to fatty acid  $\beta$ -oxidation and, therefore, it may be toxic to glycolysis-dependent brain tumor cells (Warburg effect). To understand metabolic basis of the anti-cancer action of fenofibrate, we analyzed extracellular acidification (ECAR) and oxygen consumption (OCR), as well as ATP production in LN-229 cells exposed to fenofibrate. Our results demonstrate that basal oxygen consumption (OCR) decreased significantly in LN-229 cells pretreated with fenofibrate for 24 hours; and, in contrast to the control cells, fenofibrate treated cells did not show any changes in the oxygen consumption following FCCP (uncoupling factor), 2-deoxyglucose (glycolysis inhibitor) or rotenone (complex I inhibitor) treatments. At the same time, treated cells demonstrated initially higher level of ECAR, possibly indicating the attempt of utilizing glycolysis to compensate for the impaired oxidative phosphorylation. Nevertheless, in response to FCCP-induced inhibition of ATP production, fenofibrate-treated cells were not able to increase or even maintain ECAR level (glycolysis). The end-point of this metabolic action was that fenofibrate treated cells demonstrated overall decrease in ATP levels, followed shortly by massive apoptosis. Further experiments indicated that fenofibrate induced nuclear translocation of FOXO3a, which was accompanied by the transcriptional activation of pro-apoptotic Bim at both mRNA and protein levels. Additional experiments are required to determine the link between fenofibrate-induced energy crisis and FOXO3a-mediated activation of apoptosis.

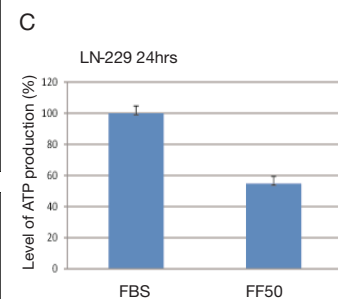
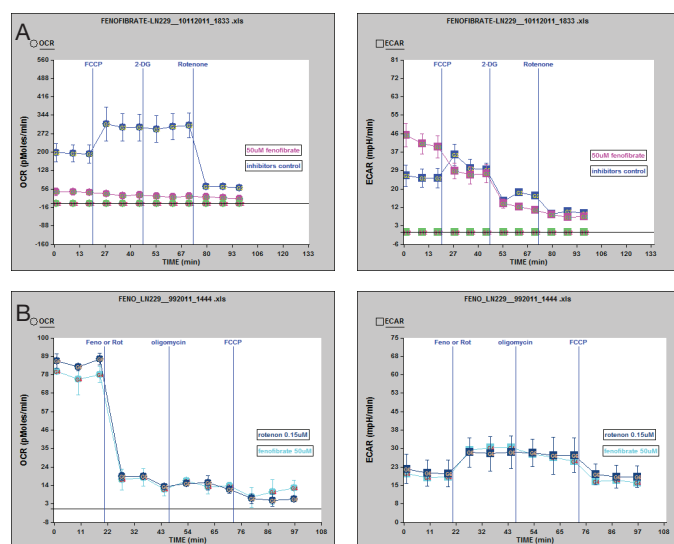


Figure 1 Validation of cellular respiration, glycolysis and ATP production in fenofibrate treated LN-229 human glioblastoma cell line.

**A) Effects of fenofibrate on basal oxygen consumption (OCR, indicates cellular respiration) and acidification (ECAR, indicates glycolysis) in LN-229 human glioblastoma cells.** To evaluate metabolic effects of 50 $\mu$ M fenofibrate on OCR and ECAR, we have employed metabolic toxins: FCCP (synthetic uncoupling factor); 2-deoxy glucose (2-DG; inhibitor of hexokinase), rotenone (inhibitor of mitochondrial complex I) and Extracellular Flux Analyzer (XF24, Seahorse Bioscience). The fenofibrate-free glioblastoma cells were characterized by the following responses: (i) addition of 0.5 $\mu$ M FCCP led to the sharp increase of OCR (oxygen consumption) due to the uncoupling of the oxidative phosphorylation from the electron transport chain, leading to ECAR increase as an attempt of ATP generation from glycolysis; (ii) injection of 20mM 2-DG inhibits glycolysis, which was not expected to affect OCR however led to sharp decrease in ECAR. (iii) Finally, the third injection, 0.3 $\mu$ M rotenone, which inhibits mitochondrial complex I resulted in OCR inhibition and could lead to the compensatory ECAR increase if the experiment would be performed in the absence of 2-DG. In comparison to these control metabolic responses, fenofibrate treated cells for 24 hours revealed dramatic difference. The most significant change was observed at the level of oxygen consumption (OCR), which was irreversibly shut down by fenofibrate. Also, differently from the control, fenofibrate treated cell were unable to activate or even maintain glycolysis (observed downregulation of ECAR) after FCCP injection, which may suggests that fenofibrate attenuates glycolytic responses.

**B) The quick response to fenofibrate.** Since fenofibrate abolished OCR in the manner similar to complex I inhibitors, we have evaluated its immediate effects on OCR and ECAR in LN-229 cells. Interestingly, fenofibrate treated cells demonstrated complete inhibition of OCR within first 5 minutes after injection, which was accompanied by a slight increase of ECAR. This acute response of LN-229 cells to fenofibrate was identical to the OCR and ECAR metabolic profiles after rotenone injection. These results suggest that fenofibrate may indeed interact with complex I, as previously postulated by Brunmair et al. (ref).

**C) ATP levels.** In parallel to the metabolic responses, we have evaluated ATP levels by ApoSensor ATP Assay Kit (BioVision). The luminometric measurement was performed using BioTek multi-plate reader. Data are presented as mean  $\pm$  SD calculated from two experiments in triplicates (n=6). Our results demonstrate that 50 M fenofibrate triggered almost 50% reduction in ATP levels at 24 hours exposure.

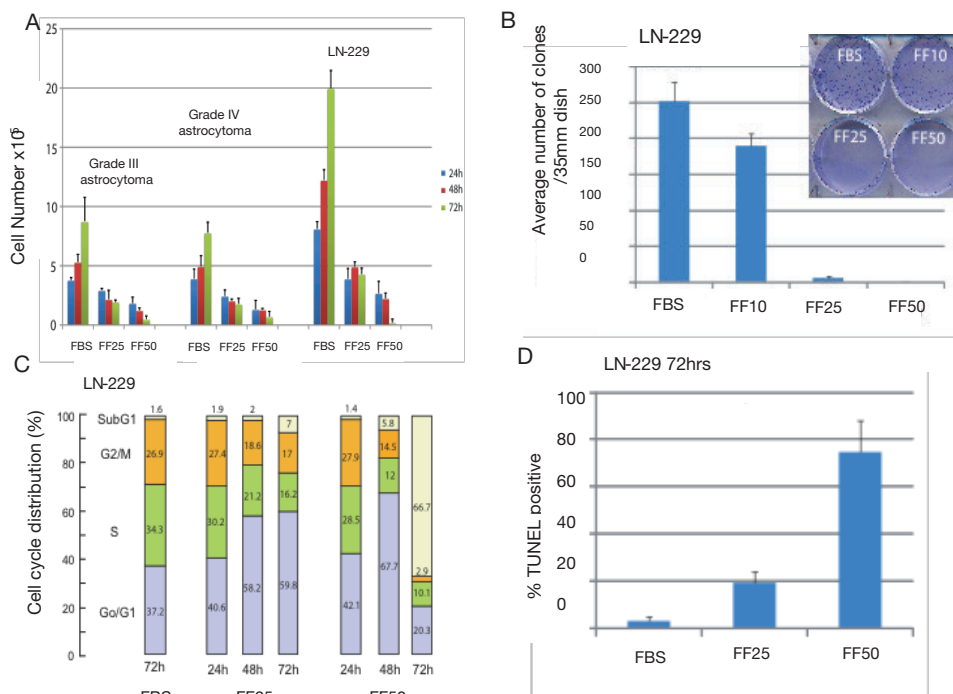


Figure 2 Effects of fenofibrate treatment on LN-229 human glioblastoma cell line and primary culture of human astrocytoma.

**A) Inhibition of proliferation.** Quantitative analysis measured by cell count of human glioblastoma cell line, and primary cultures from patients diagnosed with grade III and grade IV astrocytomas. Cells were untreated or treated with fenofibrate at the concentration of 25 $\mu$ M or 50 $\mu$ M for 24, 42, and 72 hours. In all three cases, proliferation ceased with 25 $\mu$ M of fenofibrate. Interestingly, 50 $\mu$ M fenofibrate caused a severe cell loss in all three cases at 72 hours of treatment.

**B) Inhibition of clonogenic growth.** Fenofibrate treatment (10 $\mu$ M, 25 $\mu$ M, and 50 $\mu$ M) was applied every 3 days for 2 weeks by changing media and adding appropriate treatment where needed. Four plates for each condition were used for the experiment. The average number of clones in our control (FBS) was 250. As the fenofibrate concentration increased, the number of clones showed an inverse relationship. At the concentration of 10 $\mu$ M fenofibrate treatment caused a growth of only 175 clones, at 25 $\mu$ M only 15 clones grew, and at 50 $\mu$ M no clones were detected.

**C) Fenofibrate affects on cell cycle distribution.** Flow cytometry analysis was performed to analyze cell cycle distribution of LN-229 human glioblastoma untreated and treated with different concentration of fenofibrate. In the control conditions, the distribution of cell populations was: 37.2% of cells in G<sub>0</sub>/G<sub>1</sub>, 34.3% in S phase, 26.9% in G<sub>2</sub>/M, and 1.6% in subG<sub>1</sub>. 25 $\mu$ M fenofibrate applied for 48 and 72 hours resulted in a partial G<sub>0</sub>/G<sub>1</sub> cell cycle arrest with no significant increase in subG<sub>1</sub> phase. Interestingly, the cell population treated with 50 $\mu$ M fenofibrate demonstrated more advanced G<sub>0</sub>/G<sub>1</sub> cell cycle arrest (67.7%) at 48 hours, followed by a massive cell death (66.7%) at 72 hours.

**D) Increase of apoptotic cell death.** LN-229 cell line was used for the evaluation of apoptotic cell death by utilizing TUNEL assays. TUNEL staining, specific for DNA damaged related apoptosis, was performed on untreated and fenofibrate (25 $\mu$ M, 50 $\mu$ M) treated cells for 72 hours. This assay shows a strong increase of apoptosis from 7% in FBS to 75% in 50 $\mu$ M fenofibrate. The data are presented as average % of TUNEL positive cells with standard deviation.

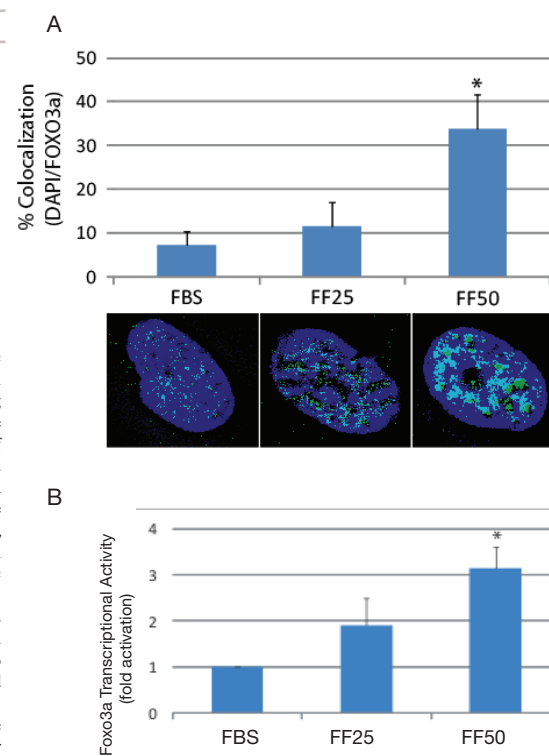


Figure 3 Effects of fenofibrate on subcellular localization and transcriptional activity of FOXO3a in human glioma cell line LN-229.

**A) Quantification analysis of FOXO3a nuclear localization** in exponentially growing LN-229 cells in the absence (FBS) and presence of fenofibrate (25 $\mu$ M and 50 $\mu$ M) treatment. The nuclear colocalization was calculated from the entire volume of the nucleus by utilizing Mask Operation included in SlideBook4 software. The data represents average number of voxels per nucleus  $\pm$  SD. \* indicates values significantly different from FBS (p<0.05). Images represent immunocytofluorescence examples of FOXO3a subcellular distribution. The cells treated with 50 $\mu$ M fenofibrate show a 30% increase of FOXO3a colocalization in the nucleus, while fenofibrate 25 $\mu$ M shows a 10% increase.

**B) Transcriptional activity of FOXO3a after treatment with fenofibrate.** Foxo3a transcriptional activity was evaluated in LN-229 cells by utilizing a dual-Firefly/Renilla luciferase reporter system and Femtomaster FB12 chemiluminometer. Data are presented as mean  $\pm$  SD calculated from two experiments in triplicates (n=6). \* indicates value statistically significantly different (p<0.05) from control (FBS; cells treated with vehicle only). Statistical significance between two measurements was determined with the two-tailed Student's t-test. In correspondence to increased colocalization of FOXO3a in the nucleus of cells treated with fenofibrate 50 $\mu$ M (A), there is also a significant increase in transcriptional activity of FOXO3a in cells kept in the same experimental conditions.

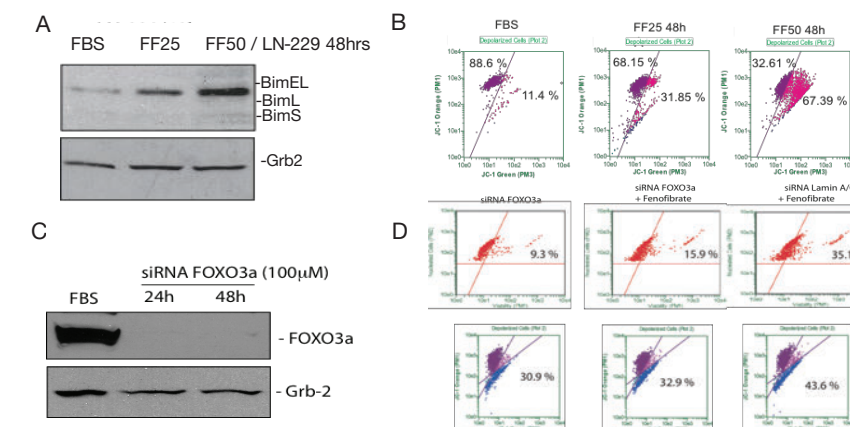


Figure 4 Fenofibrate induced FOXO3a dependant response of human glioma cell line LN-229.

**A) Effects of fenofibrate on Bim expression.** Western blot analysis showing Bim-EL, BimL, BimS, and Grb-2 protein levels in three different conditions (FBS, 25 $\mu$ M, 50 $\mu$ M fenofibrate) after 48 hours. BimEL expression is upregulated in fenofibrate 25 $\mu$ M while BimL and BimS did not show upregulation. Fenofibrate at 50 $\mu$ M showed significant upregulation in BimEL and modest upregulation of BimL and BimS.

**B) Characterization of mitochondrial potential after treatment with fenofibrate.** Mitopotential analysis was performed to investigate whether upregulated levels of Bim affect mitochondrial membrane potential. LN-229 cells were untreated or treated with 25 $\mu$ M or 50 $\mu$ M fenofibrate for 48 hours. A gradual increase in JC-1 green fluorescence and loss of orange fluorescence represents cells with compromised mitochondrial membrane potential. As shown, the percentage of LN-229 cells with compromised mitochondria reached 31.85% in the presence of 25 $\mu$ M and 67.39% with 50 $\mu$ M fenofibrate, while in the control conditions just 11.4% of cells had non-functional mitochondria.

**C, D) Effect of siRNA against Foxo3a on cell viability and mitopotential.** Western blot analysis showing FOXO3a expression and GRB-2 in FBS as well as cells treated with 100 $\mu$ M siRNA FOXO3a for 24 and 48 hours. Viacount analysis to quantify viability of cells and mitopotential analysis were performed in cells treated for 48 hours with siRNA FOXO3a, siRNA FOXO3a + fenofibrate 50 $\mu$ M, and siRNA lamin A/C + fenofibrate 50 $\mu$ M. These results show that in the presence of siRNA FOXO3a cells are partially rescued from Bim-induced apoptosis, when compared to cells treated with siRNA Lamin A/C.

**In Conclusion:** Several reports including our own research indicate that fenofibrate which is a potent agonist of PPAR $\alpha$  has strong anti-cancer properties. Our results demonstrate that fenofibrate acting at the level of energy metabolism triggers severe energy depletion in glioblastoma cells *in vitro*. Further experiments indicate that fenofibrate-induced inhibition of mitochondrial respiration is responsible for FOXO3a nuclear translocation, increase in expression of FOXO3a-dependent pro-apoptotic Bim and induction of apoptosis.

\* Ref. Brunmair B. et al. Fenofibrate impairs rat mitochondrial function by inhibition of respiratory complex I. The Journal of Pharmacology and Experimental Therapeutics, 2004